Synthetic Charge-Invertible Polymer for Rapid and Complete Implantation of Layer-by-Layer Microneedle Drug Films for Enhanced Transdermal Vaccination

Yanpu He[1,2,#], Celestine Hong[1,2,#], Jiahe Li[1,2], MayLin T Howard[1,2], Yingzhong Li[1,3], Michelle E Turvey[4], Divakara SSM Uppu[4], John R Martin[1,2], Ketian Zhang[1,5], Darrell J Irvine[1,3,5,6], and Paula T Hammond[1,2]*

[1]Koch Institute for Integrative Cancer Research, Massachusetts Institute of Technology, Cambridge, MA 02139, United States.

[2]Department of Chemical Engineering, Massachusetts Institute of Technology, Cambridge, MA 02139, United States.

[3]Department of Biological Engineering, Massachusetts Institute of Technology, Cambridge, MA 02139, United States.

[4]Infectious Diseases Interdisciplinary Research Group, Singapore-MIT Alliance for Research and Technology (SMART), Singapore, Singapore.

[5]Department of Materials Science and Engineering, Massachusetts Institute of Technology, Cambridge, MA 02139, United States.

[6]Howard Hughes Medical Institute, Chevy Chase, Maryland 20815, United States.

[*]Correspondence:

David H. Koch Professor in Engineering, Bayer Chair Professor of Chemical Engineering, Massachusetts Institute of Technology, 77 Massachusetts Avenue, Cambridge, MA 02139, United States. Email: hammond@mit.edu

Key words: polymer synthesis, layer-by-layer assembly, drug delivery, microneedle, vaccine

Abstract

The utility of layer-by-layer (LbL) coated microneedle (MN) skin patches for transdermal drug delivery has been proven a promising approach, with advantages over hypodermal injection due to painless and easy self-administration. However, the long epidermal application time required for drug implantation by existing LbL MN strategies (15 to 90 minutes) can lead to potential medication noncompliance. Here, we developed a MN platform to shorten the application time in MN therapies based on a synthetic pH-induced charge-invertible polymer poly(2-(diisopropylamino) ethyl methacrylate-*b*-methacrylic acid) (PDM), requiring only 1-minute skin insertion time to implant LbL films *in vivo*. Following MN-mediated delivery of 0.5 μg model antigen chicken ovalbumin (OVA) in the skin of mice, this system achieved sustained release over 3 days and led to an elevated immune response as demonstrated by significantly higher humoral immunity compared with OVA administration *via* conventional routes (subcutaneously and intramuscularly). Moreover, in an *ex vivo* experiment on human skin, we achieved efficient immune activation through MN-delivered LbL films, demonstrated by a rapid uptake of vaccine adjuvants by the antigen presenting cells. These features—rapid administration and the ability to elicit a robust immune response—can potentially enable a broad application of microneedle-based vaccination technologies.

Over the past several years, the technique of electrostatic layer-by-layer (LbL) assembly has enabled the production of thin polyelectrolyte multi-layer microneedles (MNs) with robust control over film structure and composition[1-5] combined with densely loaded and stabilized biological cargoes. A broad range of drugs have been investigated with LbL-coated surface mediated therapies including nucleic acids,[2,3] proteins,[6] inactivated viruses[7] and small molecule compounds.[8] Compared to traditional syringe injections, MNs offer a number of advantages by substantially reducing the risks of needle reuse, accidental needle-associated injuries, and the spread of blood-borne pathogens while allowing for pain-free self-administration.[9,10] One limitation of current LbL MN therapies is the slow detachment rate of drug-loaded LbL films from the MN surface, necessitating a relatively long period of epidermal insertion time.[2,11-13] For instance, one approach is to chemically modify the MN surface prior to LbL film deposition with pyridine functionalities, which, with an acid disassociation constant (pK_a) of 6.9, are positively charged in mildly acidic environments. Upon introduction to physiological conditions at pH 7.4, the underlying positive charges diminishes from deprotonation and the support for film construction is gradually lost, leading to detachment of the LbL film over approximately 90 minutes [**Figure 1B(i)**].[11] Another recent study coated the MN surface with a synthetic polymer containing carboxylic acid moieties; with LbL film construction at pH 5, the surface-coated acid groups are sufficiently charged to allow for subsequent film deposition, but remain insoluble in the slightly acidic environment. Upon dermal application, the exposure to plasma at pH 7.4 leads to an increased degree of polymer ionization and aqueous solubility, leading to LbL film lift-off from the MN surface after about 15 minutes [**Figure 1B(ii)**].[12] These relatively lengthy application periods lead to significant inconvenience in administrating MN therapeutics, diminishing the potential practical utility of these systems in the clinic from the perspective of medication

compliance. And while various rapid implantation strategies for dissolvable MN have been developed[14,15] over the years, a fast and complete lift-off strategy for therapeutic-coated, non-dissolvable microneedles is still currently lacking.

Herein, we devised a 1-minute lift-off platform for LbL MNs based on synthetic charge-invertible polymers that performed far more efficiently than any previously reported LbL MN systems. The polymer charge inversion occurs through the formation of cationic micellar nanoparticles at acidic pH, which switch to negatively charged micelles as physiological pH is approached. These underlying LbL lift-off coatings are constructed at mildly acidic pH and employ the charge-invertible polymer as the initial base layer to facilitate LbL film growth, but jettison the outer LbL construct through electrostatic repulsion upon exposure to the skin's physiological pH [**Figure 1B(iii)**]. To demonstrate the effectiveness of this system, these coatings have been employed to rapidly deliver LbL-encapsulated protein antigens from surface-coated MNs in order to elicit a sustained and robust therapeutic response in a minimally-invasive murine vaccination model.

Results and Discussion

Strategy for LbL Film Lift-off with Charge-invertible Polymers: The reason why layer-by-layer films have difficulty detaching from a coated surface is because they are "sticky" — each adjacent layer carries opposite charge that holds the film together through strong electrostatic interactions. State-of-the-art methods in LbL lift-off either rely on slightly decreasing the positive charge upon the microneedle surface to weaken this interaction, or increasing the degree of negative charge to enhance the solubility of the polymer base layer.[11,12] These methods, though workable, are significantly hampered by the fact that adjacent layers remain electrostatically attracted to one another, though perhaps to a lesser degree. While the proposed mechanism of this

charge-invertible lift-off polymer likewise relies on a pH-dependent change in charge, three consecutive negatively-charged layers (the oxygen plasma-treated surface, charge-invertible polymer layer, and the polyanion layer) are rapidly formed and then actively separated by a repulsive electric field, as opposed to merely compromising the LbL film integrity to slowly disengage.

To achieve charge inversion, we designed a dual-pH-sensitive diblock copolymer, synthesized *via* reversible addition-fragmentation chain-transfer polymerization[16] (RAFT)—poly(2-(diisopropylamino) ethyl methacrylate-*b*-methacrylic acid) (PDM)—which carries a positive surface charge at pH below 5.8 and negative charge above pH 5.8. The MN surface was first treated with oxygen plasma to generate a negatively charged surface and allow for the layering of positively charged PDM at a mildly acidic pH below 5.8, followed by alternating deposition of polyanions and polycations. Upon dermal insertion, the PDM layer underwent instant charge inversion after the pH shifted into that of the physiological environment, which resulted in three consecutive layers of negative charge that strongly repelled one another and rapidly detached the LbL film from the microneedle surface as demonstrated in **Figure 1B(iii)**.

RAFT Polymerization of PDM: The diblock copolymer poly(2-(diisopropylamino) ethyl methacrylate-*b*-methacrylic acid) (PDM) was synthesized *via* a one-pot reversible addition-fragmentation chain-transfer (RAFT) polymerization using 4-((((2-carboxyethyl)thio)carbonothioyl)thio)-4-cyanopentanoic acid as the chain transfer agent (CTA) and azobisisobutyronitrile (AIBN) as the initiator. To minimize potential chain transfer to the solvent, the first block was synthesized in bulk 2-(diisopropylamino) ethyl methacrylate (DPAEMA) monomers. At 60% conversion of DPAEMA as determined from ^{1}H nuclear magnetic resonance (NMR), a nitrogen-purged mixture of methacrylic acid (MAA) monomer in large excess

was injected into the reaction mixture. **Figure 2C and D** show the first-order kinetic curve of DPAEMA and MAA monomer conversion, respectively, the linearity of which implying fast initiation and insignificant chain termination during growth. The reaction was allowed to proceed for another 20 minutes and stopped with the second block having an MAA composition of 96%, with the remaining 4% repeat units being DPAEMA (**Figure 2B**). While a two-pot synthesis would be possible, the one-pot method was primarily selected to simplify the synthesis and avoid the demanding process of macro-CTA purification for re-initiation of a second polymerization. Furthermore, MAA's relatively fast polymerization kinetics compared with DPAEMA (**Figure 2B**) naturally limits DPAEMA incorporation into the second block, thus ensuring a negligible impact on the overall charge-inverting character of this material.

Micellar Behavior of PDM upon Charge-inversion: In the pH range of interest for LbL film construction and *in vivo* delivery, PDM undergoes charge inversion and forms micellar nanoparticles. The one-pot RAFT synthesized PDM diblock copolymer contains carboxylic acid functionalities in one block and tertiary alkyl amine moieties in the other. These components are chosen such that the pK_a of carboxylic acid and the pK_a of the tertiary alkyl amine's conjugated acid, respectively, coincide at around pH = 5.8. As illustrated in **Figure 3A**, in a mildly acidic aqueous solution with pH below 5.8 the DPAEMA block is highly protonated and hydrophilic while the MAA block is uncharged and hydrophobic. Due to this amphiphilic nature, PDM molecules self-assemble into micelles with the DPAEMA-containing polymer block presenting as the positively charged corona. As the pH is increased, the DPAEMA corona is gradually deprotonated and the zeta potential becomes less positive until its isoelectric point at pH 5.8. Beyond that point, deprotonation and negative charge accumulation of the MAA carboxylic acid moieties continues, eventually causing the now hydrophilic MAA block to rearrange as the micelle

corona while shifting the now hydrophobic DPAEMA block into the nanoparticle core. Dynamic light scattering measurements indicate that with the exception of the isoelectric pH, the particles are generally stabilized by either positive or negative charge and achieve diameters of about 200 nm (**Figure 3C**)**.** In conjunction with the zeta potential titration curve (**Figure 3D**) and the transmission electron microscopy (TEM) micrograph of PDM in aqueous solution of pH 5.1 and 6.5, respectively (**Figure 3E**), the charge-invertible micelle structure[17-19] proposed in **Figure 3B** is confirmed.

We noted that the micellar structure of PDM was no longer observed at pH values lower than 4.5 or higher than 7.0, as concluded from DLS and TEM measurements. TEM micrographs of PDM aqueous solutions showed no evidence of micelles at pH 4.2 and 7.5 (**Supporting Information, Figure S1**). We speculate that at those conditions, the charged polymer segment would be so charged and hydrophilic that the polymer molecule would overall favor dissolution as unimers rather than self-assembly into micelles. While it is difficult to know whether or not the polymer's conformation upon release *in vivo* is its equilibrium micellar state, its charge-inverting character (which exists in both micellar and free polymer form) would regardless enable an efficient LbL film lift off.

Surface-coated PDM Supports Steady LbL Film Growth and Protein Drug Incorporation: As the TEM images and zeta-potential titration curve (**Figure 3C and E**) demonstrate, PDM exists as positively charged micelle particles around pH 5. To demonstrate the LbL-compatibility of these positively charged nanostructures, PDM were coated onto model silicon wafers at pH 5 and used to build subsequent LbL electrostatic multilayers (**Figure 4A**). The silicon substrates were pre-treated with oxygen plasma to generate negatively charged functional groups on the surface and allow for PDM absorption. Subsequent iterative deposition

of a cationic protein lysozyme (Lys) and a polyanion poly(acrylic acid) (PAA) resulted in similar growth curves of film thickness and roughness, and amount of lysozyme protein incorporation (**Figure 4B-E, Supporting Information, Figure S2**) as reported in other lysozyme/PAA LbL film deposition studies.[12,20] One advantage this system possesses in comparison with other state-of-the-art carboxylic acid-containing polymers[2,12] is that it can support the construction of LbL films at any pH below 5.8. Specifically, for polymers only containing carboxylic acid groups, the pH where the polymer has sufficient negative charge to support an LbL film but stays insoluble in water is around 5, largely limiting its capability to encapsulate polypeptides with more acidic isoelectric points.

PDM Implants Microneedle LbL film in the Skin for Sustained Release of Drug and Efficient Immune Activation: For *in vivo* investigation of the PDM system, we synthesized an N-substituted polyaspartamide polyelectrolyte (**Supporting Information, Figure S3**) poly(N''-{N'-[N-(3-aminopropyl)-2-aminoethyl]-3-aminopropyl}aspartamide) [PAsp(EDDPA)] to serve as a biocompatible, LbL-amenable polymer for the delivery of our model antigen chicken ovalbumin (OVA). N-substituted polyaspartamides have been extensively studied in a variety of contexts related to drug delivery as complementary polycation carriers.[21-28] [PAsp(EDDPA)/Cy5-OVA] polyelectrolyte multilayers were constructed on the surface of a poly(L-lactic acid) (PLLA) microneedle patches (each patch contains 77 pyramidal microneedles, which are 650 μm in height with a square base of 250 μm × 250 μm, **Supporting Information, Figure S4**) pretreated with oxygen plasma and PDM adsorption at pH 5. To confirm stable incorporation of OVA into the LbL film and total implantation into mouse dermis, confocal micrographs of Cy5-OVA coated microneedles following 1 min application (**Figure 5B**) and the mouse dermis (**Figure 5D**) after 15 s, 30 s, and 60 s of Cy5-OVA microneedle insertion were collected. These images, together with

the cell viability assay of relevant PDM concentrations (**Supporting Information, Figure S5**) illustrated the safe and rapid, PDM-mediated release of cargo from the MN surface (**Figure 5B**) and the corresponding deposition of the LbL drug film incorporating the labelled antigen into the skin as the penetration pattern shown in **Figure 5C**. We thus concluded that 1 minute was a sufficient time to deliver the MN LbL film into the mouse dermis.

MN-mediated antigen delivery in the ear sustained the release of OVA over three days (**Figure 5E and F**), while the compound subcutaneously administered in the ear was almost completely cleared within 24 h. We speculate that the abundant Langerhans cells in the epidermis play a critical role in the uptake and presentation of OVA antigen.[29] Prior studies using similar LbL microneedle platforms have shown that MHC II^+ cells were recruited to the site of application and co-localized with the antigen in a membrane-extended form, suggesting active phagocytosis.[2,30] As shown in **Figure 5G,** we further applied LbL MN patches coated with tetramethylrhodamine (TMR) labeled polyinosinic-polycytidylic acid (poly I:C) to pieces of human skin tissue obtained from plastic surgery *ex vivo*. Two hours post-MN administration, cells were isolated from skin tissue for flow cytometry analysis. Antigen-presenting cells (APC) were gated based on $CD45^+$ $CD14^+$ and $HLA\text{-}DR^+$. Significant APC uptake of the vaccine adjuvant was observed in PDM-coated MNs, in contrast to the non-coated MN control (**Figure 5H and I**). Sustained APC uptake- mediated immune activation could potentially elicit a more robust immune response than one resulting from the bolus delivery of antigens.[31]

***In Vivo* Microneedle-delivered OVA Vaccination Induces Strong Immune Response:** Finally, we evaluated the immune response elicited against OVA antigens delivered from microneedle-deposited LbL films. A similar film architecture was used to build PDM-LbL microneedles loaded with OVA (**Figure 6A**). Groups of C57BL/6 mice were immunized on day

zero with 0.5 μg of OVA *via* microneedles, intramuscular injection or subcutaneous injection, followed by two boosts of the same dosage on day 14 and day 21 (**Figure 6B**). Sera were collected on day 28 for enzyme-linked immunosorbent assay (ELISA). Microneedle vaccination promoted a robust IgG_1-based antigen-specific immune response, generating a 9-fold and 160-fold greater antibody load compared to intramuscular and subcutaneous injections, respectively (**Figure 6C**). These data demonstrate that the PDM-enabled rapid LbL film lift-off and implantation of antigen-containing LbL films mediates sustained antigen delivery *in vivo*, thus enhancing immune activation and humoral responses in this model system.

Conclusion

It is highly desirable to develop an LbL MN platform that delivers drug with minimal application time. To this end, we incorporated a synthetic charge-invertible polymer PDM as the base layer of LbL MNs, enabling the rapid lifting-off and implanting of LbL drug films into the skin after only a 1-minute epidermal application time. To the best of our knowledge, this work presents a framework for MN design using an LbL film lift-off strategy that brings this technology much closer to translation and significantly outperforms previously reported methods by utilizing materials synthesized *via* an efficient and cost-effective one-step synthesis. The characterization and synthesis presented herein also provide insight into the molecular driving forces of rapid LbL film detachment which may inform other modes of film disassembly or release.

Applying this strategy, we generated layer-by-layer coated microneedles to deliver a model vaccine antigen, OVA. Following microneedle application to mouse ear skin for one minute, the LbL films were completely transferred from the microneedle surface onto the epidermis. Sustained release of OVA from the implanted LbL films was observed over 3 days *in vivo*, and a robust immune response was promoted *via* the microneedle-delivered OVA LbL film. Serum OVA-

specific IgG_1 levels of the microneedle vaccinated group was 9-fold and 160-fold higher than intramuscular and subcutaneous injection groups, respectively. Moreover, we demonstrated PDM microneedles on surgical samples of human skin tissue *ex vivo* followed by significant APC uptake of vaccine adjuvant delivered, suggesting the potential of applying this strategy to human subcutaneous vaccination. This platform can potentially augment delivery of other protein vaccines against viral infections and cancer. In addition, future work may also incorporate nucleic acid-based vaccines (*e.g.* messenger RNA), immune adjuvants (*e.g.* CpG oligodeoxynucleotides), and/or immune checkpoint inhibitors (*e.g.* anti-programmed cell death protein 1) into this system to compare against current delivery technologies. Finally, the approach demonstrated here could enable other technologies involving rapid film lift-off of electrostatic thin films such as wound dressings, application of medication patches, and localized transfer of therapeutic films in surgical applications.

Methods and Materials

Materials

2-(Diisopropylamino) ethyl methacrylate (DPAEMA, 97%) and methacrylic acid (MAA) were obtained from Sigma-Aldrich (St. Louis, MO, USA) and passed through a basic alumina column to remove inhibitors before polymerization. 2,2'-Azobis(2-methyl-propionitrile) (AIBN, 98%), 4-((((2-carboxyethyl)thio)carbonothioyl)thio)-4-cyanopentanoic acid (95%), lysozyme (Lys, from chicken egg, >90%), 3,3'-ethylenediiminodipropylamine (EDDPA) (94%), hexamethyldisilazane (HMDS, >99%), and other solvents were obtained from Sigma-Aldrich and used as received. β-benzyl L-aspartic acid N-carboxyanhydride (BLA-NCA) was obtained from Toronto Research Chemicals (Toronto, ON, Canada). Poly(acrylic acid) (M_w ~ 50,000, 25% aqueous solution) was obtained from Polysciences, Inc.

Synthesis of PDM: PDM was synthesized *via* a one-pot RAFT reaction. DPAEMA (648 μL) was purified by passing through activated aluminum oxide column (basic) and combined with AIBN (1.5 mg), dimethyl sulfoxide (DMSO 50 μL, as internal standard for quantitative NMR), and 4-((((2-carboxyethyl)thio)carbonothioyl)thio)-4-cyanopentanoic acid (5.6 mg) and added into a dry Schlenk flask. The flask was purged with nitrogen for 30 minutes to remove dissolved oxygen then sealed and immersed in 60 °C oil bath with magnetic stirring. During the reaction, MAA (4.6 mL) and DMF (2 mL) were combined in a 20 mL scintillation vial and bubbled with nitrogen for 30 minutes. After 2.5 hours of reaction time, the purged mixture of MAA and DMF was added into the Schlenk flask with a nitrogen-purged syringe. The flask was briefly removed from the oil bath, vortexed to mix thoroughly, and returned to the oil bath to allow the reaction to continue at 60 °C for another 20 minutes. Samples were withdrawn from the reaction mixture at various time intervals and diluted in deuterated chloroform for ^{1}H nuclear magnetic resonance (NMR) analysis of monomer consumption.

20 minutes after the addition of MAA and DMF, the reaction was terminated by removing the glass stopper on Schlenk flask, exposing the solution to air. The reaction mixture was diluted with DMF and precipitated in cold diethyl ether (0 °C) before re-dissolution in water. The aqueous solution was then adjusted to pH ~ 8 with a sodium hydroxide aqueous solution and centrifuged at 2000 rcf for 5 minutes to precipitate the poly(DPAEMA) dead chains. The supernatant was dialyzed (M_w cut-off: 6-8kDa) in water for 24 hours, and freeze-dried *in vacuo* to give a white powder (124 mg, M_n ~ 38,000, M_w/M_n = 1.10). ^{1}H NMR (400 MHz, D_2O) pMAA block: δ 0.89 – 1.05 (s, 3H), 1.36 – 1.48 (s, 2H). pDPAEMA block: δ 1.05 – 1.15 (s, 3H), 1.64 – 1.93 (d, 14H), 3.37 – 3.63 (t, 2H), 3.68 – 3.93 (m, 2H), 4.19 – 4.53 (t, 2H).

Synthesis of PAsp(EDDPA): PAsp(EDDPA) synthesis was modified from literature.[21-24,32] Briefly, in the nitrogen glove box, BLA-NCA (250 mg) and HMDS (5.4 mg) as initiator were first dissolved in nitrogen purged anhydrous DMF (2.5 mL in total) separately, then combined and stirred at room temperature under a stream of nitrogen for 48 hours. The reaction mixture was precipitated in cold (0 °C) diethyl ether and re-dissolved in dichloromethane (DCM) for three times, then dried *in vacuo* overnight for use (158 mg).

Dried poly(β-benzyl L-aspartic acid) (PBLA) backbone was dissolved in anhydrous 1-methyl-2-pyrrolidinone (NMP) at 100 mg/mL and brought to 0°C together with 4 mL 2-fold diluted EDDPA solution in NMP. The EDDPA solution was then added dropwise into the stirring PBLA solution in a glass vial. The vial was then sealed and allowed to react for 3 hours. The resulting reaction mixture was mixed with 4 mL 1 N hydrochloric acid (HCl) and dialyzed at 0°C against 0.1 N HCl for 24 hours, then against water for another 24 hours and finally freeze-dried *in vacuo* to give a white powder (110 mg, M_n ~ 81,000, M_w/M_n = 1.04). ^{1}H NMR (400 MHz, D_2O) δ 1.54 – 1.80 (m, 4H), 2.44 – 2.90 (m, 12H), 3.08 – 3.24 (m, 2H), 3.24 – 3.34 (m, 1H), 4.55 – 4.67 (s, 1H).

PLLA microneedle fabrication: To fabricate microneedle patches, pellets of poly(L-lactide) (PLLA) were placed over poly(dimethylsiloxane) (PDMS) negative molds and melted under vacuum by gradually heating to 200 °C. The oven was then vented slowly, allowing atmospheric pressure to pack liquid PLLA into the PDMS molds. The molds were then transferred to the fridge when they reached room temperature and cooled at -20 °C for 1 hr. Finally, the molds were returned to room temperature and PLLA microneedles were de-molded for use.

PDM layer deposition: Prior to deposition of PDM on microneedle patches and Si water, the surfaces were first treated with oxygen plasma for 10 minutes (18 W oxygen plasma produced

by a PDC-32G plasma cleaner). The treated surfaces were then immersed in PDM solution (1 mg/mL in 10 mM sodium acetate buffer) for 15 minutes and rinsed with 10 mM sodium acetate buffer for 30 seconds with agitation before LbL dipping.

LbL film construction: LbL films on microneedles and Si wafers were constructed with a Zeiss HMS-D250 Serial Stainer. PDM-coated microneedles or Si wafers were processed with 40 alternating 20-minute immersions in lysozyme, ovalbumin or Cy5-labelled ovalbumin, and polyamine or poly(acrylic acid) solution. The concentrations of both polycation and polyanion were 1 mg/mL in pH 5.4 10 mM sodium acetate buffer, separated by three 30-second rinse steps in 10 mM sodium acetate buffer (pH 5.4). Another set of PDM-coated Si wafers were treated with alternating 5-minute immersions in lysozyme (1 mg/mL) and PAA (1 mg/mL) solutions in 10 mM sodium acetate buffer (pH 5.1), with each dip separated by two 30-second wash steps in 10 mM sodium acetate buffer (pH 5.1).

PolyI:C LbL coated microneedles for human skin were prepared using the StratoSequence VI from nanoStrata Inc. (USA) with spinning (100-120 rpm)[12]. PDM-coated PLLA microneedles were secured in a holder prior to immersion in the polymer solutions. Fluorescent PolyI:C (HMW, InvivoGen) was prepared using tetramethylrhodamine (TMR) Label-IT reagent (Mirus Bio). Poly1 (M_w ~9.8 kDa, PDI = 1.2), a degradable poly(amino ester) synthesized as modified from literature,[33,34,35] was dissolved in 0.1 M sodium acetate buffer and PolyI:C in PBS adjusted to pH = 5.5. $(Poly1/TMR\text{-}PolyI:C)_{40}$ films were assembled at pH = 5.5 with spinning through alternative immersion into Poly1 (1 mg/mL) and TMR-PolyI:C (40 µg/mL) for 5 minutes, separated by two 30-second wash steps in pH = 5.5 PBS.

***In vitro* release study of LbL film for drug load determination:** Silicon chips coated with $(PDM/PAA)_1$ $(lysozyme/PAA)_n$ LbL films were measured with a ruler to determine the

surface area of the film. They were then immersed in room-temperature phosphate buffer saline (PBS) in low-bind, 2 mL Eppendorf microcentrifuge tubes for 1 minute to allow the films to be lifted-off from the surface. The silicon chips were inspected visually upon removal. If small pieces of lifted-off LBL film had clung to the surface of the chip, they were gently rinsed back into the tube with the release media. Since the lysozyme-containing LbL film was lifted-off, but not degraded in the 1-minute time span, the release aliquots were stored at 4°C for 72 hours before measuring lysozyme concentration to allow the lysozyme in the lifted-off film pieces to diffuse into the release media.

Lifted-off film aliquots were compared to standards made of lysozyme (purchased from Sigma Aldrich, CAS# 12650-88-3) in PBS. A PierceTM BCA Protein Assay Kit (CAS# 23225, purchased from ThermoFisher Scientific) assay was used to quantify concentration of lysozyme according to the manufacturer's instructions. The mass of lysozyme contained in each film was normalized by the surface area of the film.

***In vivo* delivery on mouse ear:** Mice studies were approved by the MIT IUCAC and mice were cared for in the USDA-inspected MIT Animal Facility under federal, state, local, and NIH guidelines for animal care. *In vivo* delivery experiments where LbL-coated microneedles were pressed into the mouse ear for 1 minute then removed were performed on anesthetized 8 weeks old female C57BL/6 mouse (Taconic Biosciences, Hudson, NY, USA). Subcutaneous and intramuscular injection dosages include the same amount of OVA and PAsp(EDDPA) polymer as in each microneedle administration.

Ethics statement: Healthy human skin tissue was obtained from abdominoplastic surgery. The studies were approved by the respective institutional review boards (National Health Group Domain Specific Review Board (NHG DSRB 2012/00928) and Singhealth

Centralized Institutional Review Board (CIRB 2011/327/E), respectively) and patients gave written informed consent. All skin samples were processed on the day of surgery. Microneedles were applied onto human skin using a spring applicator (Micropoint Technologies Pte Ltd., Singapore).

Flow cytometry analysis of human skin tissue *ex vivo* antigen presentation: After microneedle application, human skin dermatome sections (300 mm) were incubated in 0.05 mg/ml DNase I (Roche) and RPMI + 10% FCS (BioWest) containing 0.8 mg/ml collagenase (Type IV, Worthington-Biochemical) for 12 hours. Following incubation, a 70 μm filter was used to obtain a single cell suspension. Cells were labeled using the following: anti-HLA-DR, anti-CD45, and anti-CD14 reagents (all BD Biosciences) with viability discrimination using DAPI. Flow cytometry was performed on an LSRII (Becton Dickinson). Software analysis was performed with FlowJo (TreeStar).

Statistical analysis: All statistical analysis were performed using GraphPad Prism 5.03 (San Diego, CA, USA). Data were analyzed with one-way ANOVA followed by Student's *t* test for statistical significance.

Author Information

Author Contributions

[#]These authors contributed equally to this work. Y.H. and C.H. designed the experiments, Y.H. and C.H. synthesized and characterized the PDM and PAsp(EDDPA) polymer, Y.H., C.H., J.L., M.T.H., Y.L., J.R.M, and K.Z. studied the LbL MN construction, drug release *in vitro*, drug delivery on mouse *in vivo* and immune response. M.E.T. and D.SSM.U. synthesized the PBAE

polymer and carried out the human skin antigen presentation experiment. P.T.H. and D.J.I. supervised the study. Y.H., C.H., and P.T.H. wrote the manuscript.

Funding

This work was supported by the Department of Defense Congressionally Directed Medical Research Programs (CDMRP) Ovarian Cancer Research Program, Singapore-MIT Alliance for Research and Technology (SMART), Cancer Center Support Grant (CCSG) Pilot Awards at David H. Koch Institute of Integrative Cancer Research at MIT, and the Institute for Solider Nanotechnologies at MIT.

Associated Contents

The authors declare no competing financial interests.

Acknowledgement

We acknowledge Dr. Dong Soo Yun at the David H. Koch Institute Nanotechnology Materials Core at MIT for providing assistance in the TEM imaging; Jeff Wyckoff at the David H. Koch Institute Microscopy Facility at MIT for providing assistance in the confocal microscope imaging.

Supporting Information

Supporting Information Available: supplementary figures, materials and methods. This material is available free of charge *via* the Internet at http://pubs.acs.org.

Figure Legends

Figure 1. Overview of state-of-the-art approaches and the current design of LbL film lift-off from microneedles. (A) Schematic view of the microneedle skin patches where drug-releasing

surface is generated. (B) Two state-of-the-art approaches utilizing (i) chemically functionalizing surface with pyridine moiety (ii) coating of a layer of polymer with carboxylic acid functional groups to support and release the LbL film on top depending on the environmental pH, and (iii) the current design of LbL film lift-off mechanism based on charge-invertible polymers.

Figure 2. Synthesis scheme and kinetic study of PDM polymer. (A) Synthesis scheme of one-pot RAFT polymerization of PDM polymer. (B) Number average monomers converted per initiator calculated from monomer consumption kinetics as determined from ^{1}H nuclear magnetic resonance. (C) First order linear kinetics of DPAEMA monomer and (D) MAA monomer consumption as determined from ^{1}H nuclear magnetic resonance.

Figure 3. Charge-invertible micellization behavior of PDM polymer. (A) Schematics of PDM's charge-invertibility with pH change, the pK_a of carboxylic acid and the pK_a of the tertiary alkyl amine's conjugated acid, respectively, coincide at around pH = 5.8. (B) Proposed schematics of charge-invertible micellization behavior. (C) Zeta-potential and (D) particle diameter measured from electrophoretic and dynamic light scattering, respectively, of 0.1 mg/mL PDM dissolved in 10mM sodium acetate buffer solution titrated from pH 5.1 to 6.8. (E) TEM images of PDM in aqueous solution at pH 5.1 and 6.5, respectively. Scale bar 200 nm.

Figure 4. LbL film growth study on PDM. (A) Film architecture schematics of (Lys/PAA) LbL film constructed on top of PDM polymer coated silicon wafer at acidic LbL assembly environment. (B) Profilometry measured LbL film thickness growth with the number of (Lys/PAA) bilayers deposited atop PDM. (C) LbL film roughness as a function of numbers of bilayers coated (n = 4). Values are reported as mean ± s.e.m. (D) BCA assay determined Lys drug loading in LbL film with the number of (Lys/PAA) bilayers deposited atop PDM coated silicon wafer (n = 3) after 1 min *in vitro* incubation in PBS. Values are reported as mean ± s.e.m. (E) Representative scanning

electron microscopy images of cross-sections of $(Lys/PAA)_{20,30,40}$ LbL film constructed on top of PDM coated silicon wafer.

Figure 5. *In vivo* mouse skin and *ex vivo* human skin implantation of LbL drug film from microneedle surface upon charge invert of PDM. (A) Film architecture schematics of $[PAsp(EDDPA)/Cy5\text{-}OVA]_{40}$ LbL coated microneedle for mouse ear. (B) Confocal micrograph of Cy5-OVA on microneedle surface before and after 1 min application in mouse dermis. Scale bar 0.5 mm. (C) Image of mouse ear skin after 1 min microneedle (PDM/Polystyrene sulfonate/methylene blue)$_1$ application showing the penetration pattern. Scale bar 2 mm. (D) Confocal micrograph of Cy5-OVA delivered onto mouse dermis after 15 s, 30 s, 60 s of microneedle insertion, respectively. Scale bar 1 mm. (E) Representative IVIS images showing Cy5 signal intensity on mouse ear at day 0, 1, 2, and 3 after MN or SC administration on left ear (right ear untreated). (F) Integrated radiant efficiency decay of Cy5-OVA on mouse ear in 3 days demonstrating *in vivo* sustained release of Cy5-OVA from PDM microneedle (MN) implanted LbL film, compared to subcutaneously (SC) injected same amount of Cy5-OVA (n = 6/group). Values are reported as mean ± s.e.m. ***p = 0.0004, as analyzed by one-way ANOVA. (G) Film architecture schematics of $[Poly1/PolyI:C\text{-}TMR]_{40}$ LbL coated microneedle for human skin tissue. Flow cytometric analysis performed on cells isolated from human skin following 2 minute microneedle application for detection of film uptake, shown as (I) proportion, and (H) representative plots of antigen presenting cells ($CD45^+$ $CD14^+$ HLA-DR^+) positive for PolyI:C-TMR LbL film; values are reported as mean ± s.e.m. **p=0.0017 unpaired t-test; numbers in plots indicate percent cells in outlined area.

Figure 6. *In vivo* OVA vaccination of LbL drug film from microneedle surface upon charge inversion of PDM. (A) Film architecture schematics of $[PAsp(EDDPA)/OVA]_{40}$ LbL coated

microneedle. (B) Vaccination dosing and ELISA schedule, each dose is 0.5 μg of OVA by either PDM-mediated microneedle, subcutaneous, or intramuscular administration. (C) Serum OVA-specific IgG_1 antibody level measured in mouse serum (n = 10/group). Values are reported as mean ± s.e.m. ***$p < 0.0001$, as analyzed by one-way ANOVA.

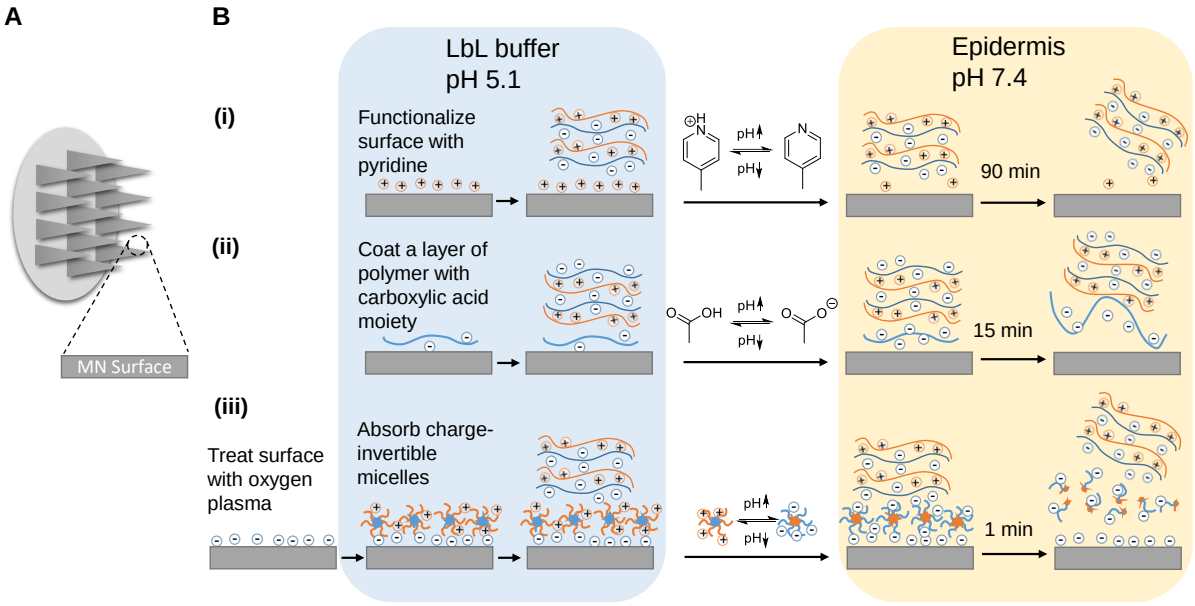
A
B
MN Surface
LbL buffer
pH 5.1
Epidermis
pH 7.4
(i)
Functionalize surface with pyridine
(ii)
Coat a layer of polymer with carboxylic acid moiety
(iii)
Treat surface with oxygen plasma
Absorb charge-invertible micelles
pH
pH
90 min
15 min
1 min

Figure 1.

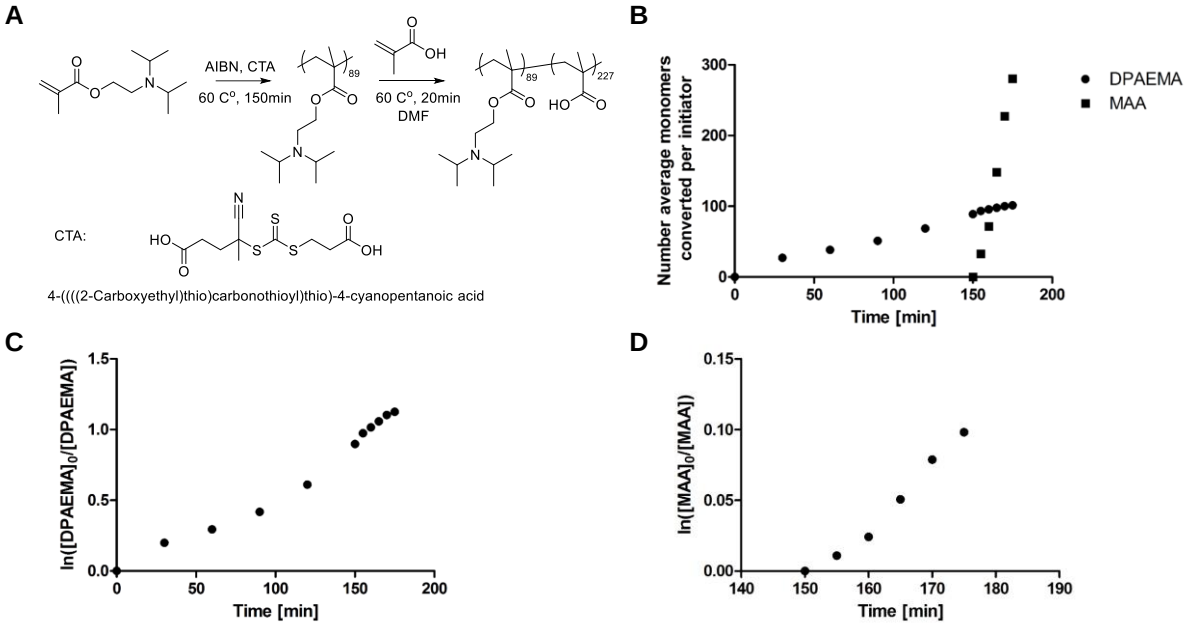
A
AIBN, CTA
60 C°, 150min
60 C°, 20min
DMF
89
227
CTA:
4-((((2-Carboxyethyl)thio)carbonothioyl)thio)-4-cyanopentanoic acid
B
Number average monomers converted per initiator
Time [min]
DPAEMA
MAA
C
ln([DPAEMA]0/[DPAEMA])
Time [min]
D
ln([MAA]0/[MAA])
Time [min]

Figure 2.

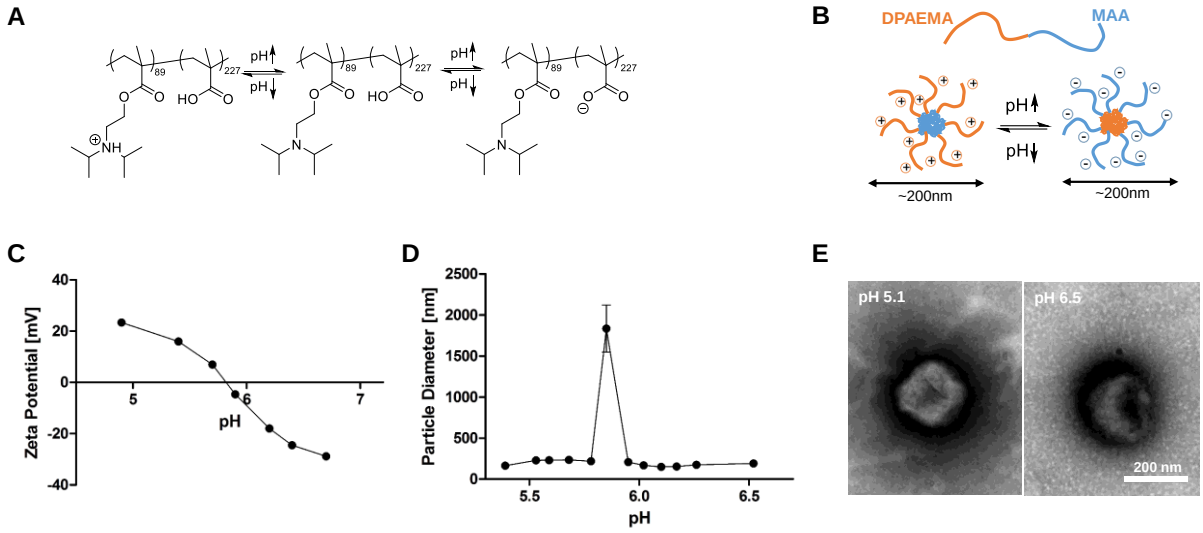
A
B
DPAEMA
MAA
pH
pH
~200nm
~200nm
C
Zeta Potential [mV]
40
20
0
-20
-40
5
6
7
pH
D
Particle Diameter [nm]
2500
2000
1500
1000
500
0
5.5
6.0
6.5
pH
E
pH 5.1
pH 6.5
200 nm

Figure 3.

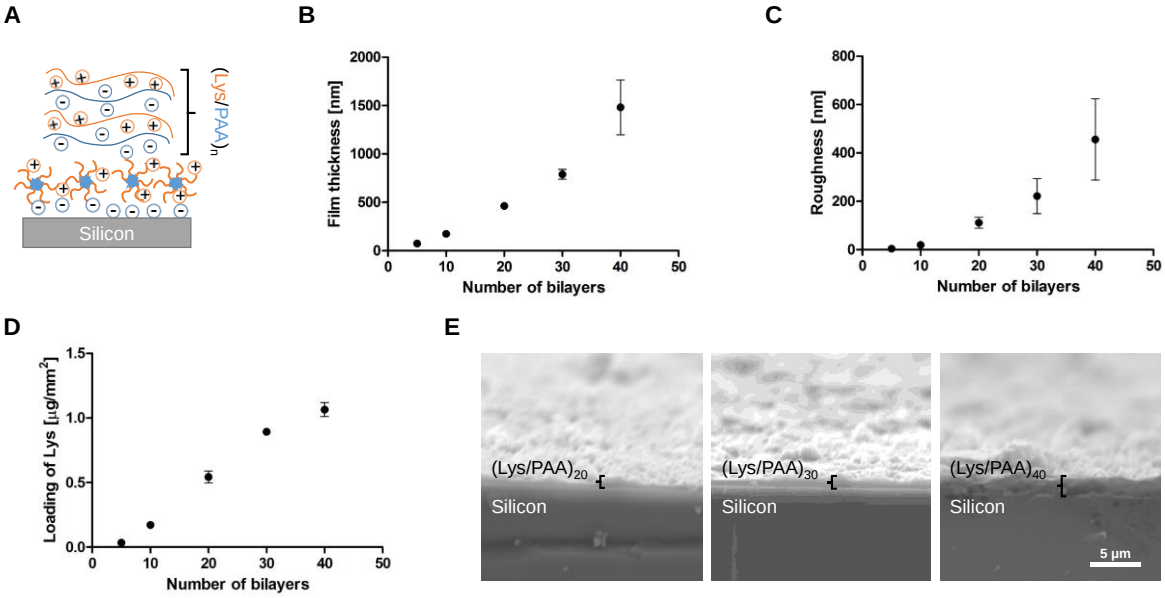
A
B
C
D
E
(Lys/PAA)n
Silicon
Film thickness [nm]
Number of bilayers
Roughness [nm]
Number of bilayers
Loading of Lys [µg/mm²]
Number of bilayers
(Lys/PAA)20
Silicon
(Lys/PAA)30
Silicon
(Lys/PAA)40
Silicon
5 µm

Figure 4.

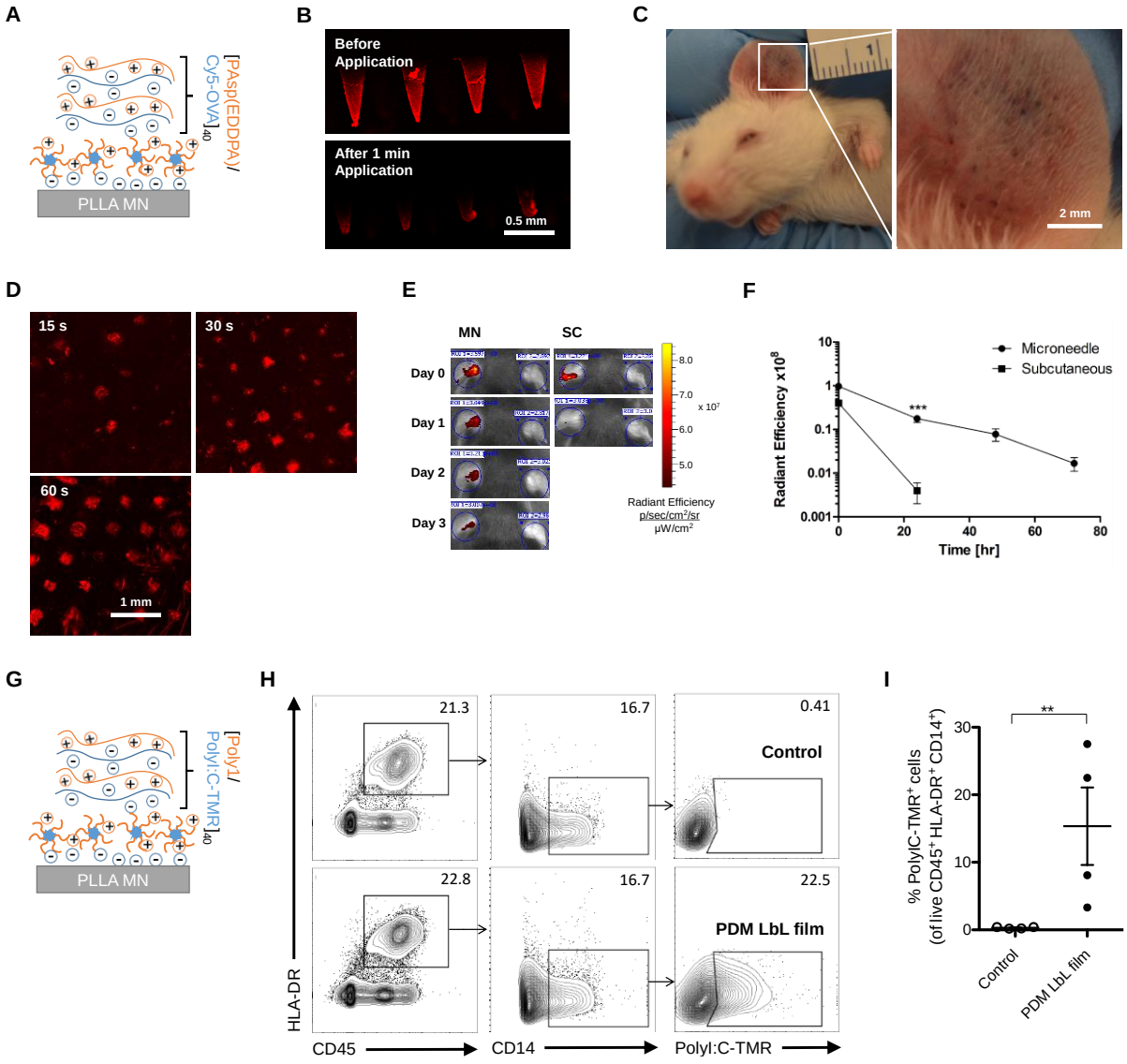
A
[Pasp(EDDPA)/Cy5-OVA]40
PLLA MN
B
Before Application
After 1 min Application
0.5 mm
C
2 mm
D
15 s
30 s
60 s
1 mm
E
MN
SC
Day 0
Day 1
Day 2
Day 3
8.0
7.0
6.0
5.0
x 10^7
Radiant Efficiency
p/sec/cm²/sr
µW/cm²
F
Radiant Efficiency x10^8
Microneedle
Subcutaneous
***
Time [hr]
G
[Poly1/Poly I:C-TMR]40
PLLA MN
H
21.3
16.7
0.41
Control
22.8
16.7
22.5
PDM LbL film
HLA-DR
CD45
CD14
Poly I:C-TMR
I
% PolyIC-TMR+ cells (of live CD45+ HLA-DR+ CD14+)
**
Control
PDM LbL film

Figure 5.

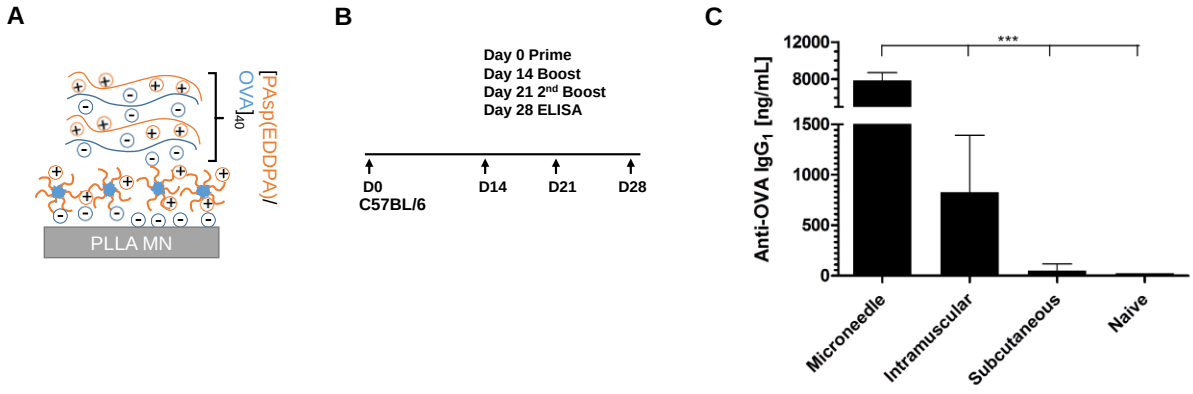
A
[PAsp(EDDPA)/OVA]40
PLLA MN
B
Day 0 Prime
Day 14 Boost
Day 21 2nd Boost
Day 28 ELISA
D0
C57BL/6
D14
D21
D28
C
***
Anti-OVA IgG1 [ng/mL]
12000
8000
1500
1000
500
0
Microneedle
Intramuscular
Subcutaneous
Naive

Figure 6.

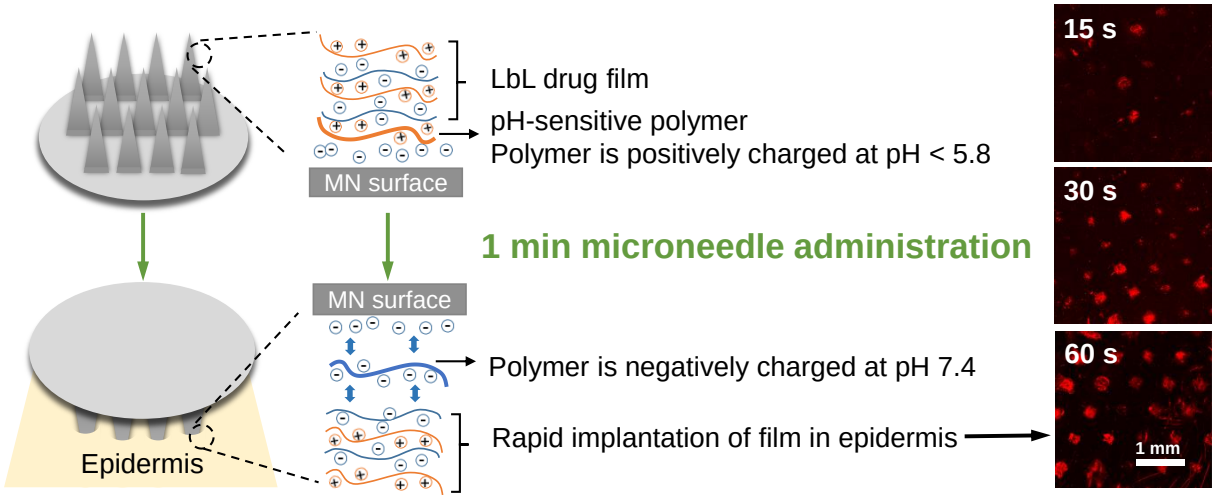

Table of Contents Figure.

References

(1) Hammond, P.T., Building Biomedical Materials Layer-by-Layer. *Mater. Today*, **2012**. *15*:196-206.

(2) DeMuth, P.C.; Y. Min; B. Huang; J.A. Kramer; A.D. Miller; D.H. Barouch; P.T. Hammond, and D.J. Irvine, Polymer Multilayer Tattooing for Enhanced DNA Vaccination. *Nat. Mater.*, **2013**. *12*:367-376.

(3) DeMuth, P.C.; X. Su; R.E. Samuel; P.T. Hammond, and D.J. Irvine, Nano‐Layered Microneedles for Transcutaneous Delivery of Polymer Nanoparticles and Plasmid DNA. *Adv. Mater.*, **2010**. *22*:4851-4856.

(4) Saurer, E.M.; R.M. Flessner; S.P. Sullivan; M.R. Prausnitz, and D.M. Lynn, Layer-by-Layer Assembly of DNA-and Protein-Containing Films on Microneedles for Drug Delivery to the Skin. *Biomacromolecules*, **2010**. *11*:3136-3143.

(5) van der Maaden, K.; W. Jiskoot, and J. Bouwstra, Microneedle Technologies for (Trans) Dermal Drug and Vaccine Delivery. *J. Controlled Release*, **2012**. *161*:645-655.

(6) Hsu, B.B.; S.R. Hagerman; K. Jamieson; J. Veselinovic; N. O'Neill; E. Holler; J.Y. Ljubimova, and P.T. Hammond, Multilayer Films Assembled from Naturally-Derived Materials for Controlled Protein Release. *Biomacromolecules*, **2014**. *15*:2049-2057.

(7) Hsu, B.B.; S.Y. Wong; P.T. Hammond; J. Chen, and A.M. Klibanov, Mechanism of Inactivation of Influenza Viruses by Immobilized Hydrophobic Polycations. *Proc. Natl. Acad. Sci.*, **2011**. *108*:61-66.

(8) Hsu, B.B.; M.-H. Park; S.R. Hagerman, and P.T. Hammond, Multimonth Controlled Small Molecule Release from Biodegradable Thin Films. *Proc. Natl. Acad. Sci.*, **2014**. *111*:12175-12180.

(9) Glenn, G.M.; R.T. Kenney; L.R. Ellingsworth; S.A. Frech; S.A. Hammond, and J.P. Zoeteweij, Transcutaneous Immunization and Immunostimulant Strategies: Capitalizing on the Immunocompetence of the Skin. *Expert Rev. Vaccines*, **2003**. *2*:253-267.

(10) Prausnitz, M.R. and R. Langer, Transdermal Drug Delivery. *Nat. Biotechnol.*, **2008**. *26*:1261.

(11) Schipper, P.; K. van der Maaden; V. Groeneveld; M. Ruigrok; S. Romeijn; S. Uleman; C. Oomens; G. Kersten; W. Jiskoot, and J. Bouwstra, Diphtheria Toxoid and N-Trimethyl Chitosan Layer-by-Layer Coated Ph-Sensitive Microneedles Induce Potent Immune Responses Upon Dermal Vaccination in Mice. *J. Controlled Release*, **2017**. *262*:28-36.

(12) He, Y.; J. Li; M.E. Turvey; M.T. Funkenbusch; C. Hong; D.S. Uppu; H. He; D.J. Irvine, and P.T. Hammond, Synthetic Lift-Off Polymer beneath Layer-by-Layer Films for Surface-Mediated Drug Delivery. *ACS Macro Lett.*, **2017**. *6*:1320-1324.

(13) Zeng, Q.; J.M. Gammon; L.H. Tostanoski; Y.-C. Chiu, and C.M. Jewell, In Vivo Expansion of Melanoma-Specific T Cells Using Microneedle Arrays Coated with Immune-Polyelectrolyte Multilayers. *ACS Biomater. Sci. Eng.*, **2016**. *3*:195-205.

(14) Chu, L.Y. and M.R. Prausnitz, Separable Arrowhead Microneedles. *J. Controlled Release*, **2011**. *149*:242-249.

(15) Zhu, D.D.; Q.L. Wang; X.B. Liu, and X.D. Guo, Rapidly Separating Microneedles for Transdermal Drug Delivery. *Acta Biomater.*, **2016**. *41*:312-319.

(16) Chiefari, J.; Y. Chong; F. Ercole; J. Krstina; J. Jeffery; T.P. Le; R.T. Mayadunne; G.F. Meijs; C.L. Moad, and G. Moad, Living Free-Radical Polymerization by Reversible Addition− Fragmentation Chain Transfer: The Raft Process. *Macromolecules*, **1998**. *31*:5559-5562.

(17) Zhang, R.; L.D. Morton; J.D. Smith; F. Gallazzi; T.A. White, and B.D. Ulery, Instructive Design of Triblock Peptide Amphiphiles for Structurally Complex Micelle Fabrication. *ACS Biomater. Sci. Eng.*, **2018**.

(18) Zhang, R.; J.D. Smith; B.N. Allen; J.S. Kramer; M. Schauflinger, and B.D. Ulery, Peptide Amphiphile Micelle Vaccine Size and Charge Influence the Host Antibody Response. *ACS Biomater. Sci. Eng.*, **2018**.

(19) Zhang, R. and B.D. Ulery, Synthetic Vaccine Characterization and Design. *J. Bionanosci.*, **2018**. *12*:1-11.

(20) Macdonald, M.; N.M. Rodriguez; R. Smith, and P.T. Hammond, Release of a Model Protein from Biodegradable Self Assembled Films for Surface Delivery Applications. *J. Controlled Release*, **2008**. *131*:228-234.

(21) Uchida, H.; K. Itaka; T. Nomoto; T. Ishii; T. Suma; M. Ikegami; K. Miyata; M. Oba; N. Nishiyama, and K. Kataoka, Modulated Protonation of Side Chain Aminoethylene Repeats in N-Substituted Polyaspartamides Promotes Mrna Transfection. *J. Am. Chem. Soc.*, **2014**. *136*:12396-12405.
(22) Li, J.; W. Wang; Y. He; Y. Li; E.Z. Yan; K. Zhang; D.J. Irvine, and P.T. Hammond, Structurally Programmed Assembly of Translation Initiation Nanoplex for Superior Mrna Delivery. *ACS Nano*, **2017**. *11*:2531-2544.
(23) Li, J.; Y. He; W. Wang; C. Wu; C. Hong, and P.T. Hammond, Polyamine-Mediated Stoichiometric Assembly of Ribonucleoproteins for Enhanced Mrna Delivery. *Angew. Chem.*, **2017**. *129*:13897-13900.
(24) Li, J.; C. Wu; W. Wang; Y. He; E. Elkayam; L. Joshua-Tor, and P.T. Hammond, Structurally Modulated Codelivery of Sirna and Argonaute 2 for Enhanced Rna Interference. *Proc. Natl. Acad. Sci.*, **2018**. *115*:E2696-E2705.
(25) Jiang, Y.; P. Arounleut; S. Rheiner; Y. Bae; A.V. Kabanov; C. Milligan, and D.S. Manickam, Sod1 Nanozyme with Reduced Toxicity and Mps Accumulation. *J. Controlled Release*, **2016**. *231*:38-49.
(26) Jiang, Y.; A.M. Brynskikh; D. S-Manickam, and A.V. Kabanov, Sod1 Nanozyme Salvages Ischemic Brain by Locally Protecting Cerebral Vasculature. *J. Controlled Release*, **2015**. *213*:36-44.
(27) Natarajan, G.; C. Perriotte-Olson; F. Bhinderwala; R. Powers; C.V. Desouza; G.A. Talmon; J. Yuhang; M.C. Zimmerman; A.V. Kabanov, and V. Saraswathi, Nanoformulated Copper/Zinc Superoxide Dismutase Exerts Differential Effects on Glucose Vs Lipid Homeostasis Depending on the Diet Composition Possibly *Via* Altered Ampk Signaling. *Translational Research*, **2017**. *188*:10-26.
(28) Efremenko, E.N.; I.V. Lyagin; N.L. Klyachko; T. Bronich; N.V. Zavyalova; Y. Jiang, and A.V. Kabanov, A Simple and Highly Effective Catalytic Nanozyme Scavenger for Organophosphorus Neurotoxins. *J. Controlled Release*, **2017**. *247*:175-181.
(29) Sparber, F.; C.H. Tripp; M. Hermann; N. Romani, and P. Stoitzner, Langerhans Cells and Dermal Dendritic Cells Capture Protein Antigens in the Skin: Possible Targets for Vaccination through the Skin. *Immunobiology*, **2010**. *215*:770-779.
(30) DeMuth, P.C.; J.J. Moon; H. Suh; P.T. Hammond, and D.J. Irvine, Releasable Layer-by-Layer Assembly of Stabilized Lipid Nanocapsules on Microneedles for Enhanced Transcutaneous Vaccine Delivery. *ACS Nano*, **2012**. *6*:8041-8051.
(31) Tam, H.H.; M.B. Melo; M. Kang; J.M. Pelet; V.M. Ruda; M.H. Foley; J.K. Hu; S. Kumari; J. Crampton, and A.D. Baldeon, Sustained Antigen Availability During Germinal Center Initiation Enhances Antibody Responses to Vaccination. *Proc. Natl. Acad. Sci.*, **2016**. *113*:E6639-E6648.
(32) Lu, H. and J. Cheng, Hexamethyldisilazane-Mediated Controlled Polymerization of A-Amino Acid N-Carboxyanhydrides. *J. Am. Chem. Soc.*, **2007**. *129*:14114-14115.
(33) Jiang, Y.; A. Gaudin; J. Zhang; T. Agarwal; E. Song; A.C. Kauffman; G.T. Tietjen; Y. Wang; Z. Jiang, and C.J. Cheng, A "Top-Down" Approach to Actuate Poly (Amine-Co-Ester) Terpolymers for Potent and Safe Mrna Delivery. *Biomaterials*, **2018**.
(34) Lynn, D.M. and R. Langer, Degradable Poly (B-Amino Esters): Synthesis, Characterization, and Self-Assembly with Plasmid DNA. *J. Am. Chem. Soc.*, **2000**. *122*:10761-10768.
(35) Wu, C.; J. Li; W. Wang, and P.T. Hammond, Rationally Designed Polycationic Carriers for Potent Polymeric Sirna-Mediated Gene Silencing. *ACS Nano*, **2018**. *12*:6504-6514.